SYNTHESIS REPORT

FOR PUBLICATION

CONTRACT N* : BREU-CT90-0347

PROJECT No : BE-3044-90

TITLE : DEVELOPMENT OF A SCANNING POSITRON MICROSCOPE FOR DEFECT ANALYSIS IN MATERIALS SCIENCE

PROJECT COORDINATOR : PROF. DR. W., TRIFTSHÄUSER
UNIVERSITÄT DER BUNDESWEHR MÜNCHEN

PARTNERS :

UNIVERSITÄT DER BUNDESWEHR MÜNCHEN
INSTITUT FÜR NUKLEARE FESTKÖRPERPHYSIK

CONSORZIO INTERUNIVERSITARIO NAZIONALE
PER LA FISICA DELLA MATERIA,
C/O UNIVERSITY DEGLI STUDI DI TRENTO
DIPARTIMENTO DI FISICA

STARTING DATE : 01/06/91 DURATION : 48 MONTHS

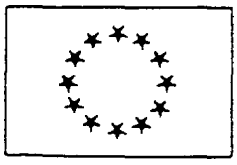

PROJECT FUNDED BY THE EUROPEAN COMMISSION UNDER THE BRITE/EURAM PROGRAMME

DATE : August 2, 1995

2. DEVELOPMENT OF A SCANNING POSITRON MICROSCOPE FOR DEFECT ANALYSIS IN MATERIALS SCIENCE

W. Triftshäuser, G. Kögel, P. Sperr, D.T. Britton, K. Uhlmann, P. Willutzki;
Institut für Nukleare Festkörperphysik, Universität der Bundeswehr Munchen,
D -85577 Neubiberg, Germany
and
G.P. Karwasz, A. Zecca, R.S. Brusa, M.P. Duarte-Naia, J. Paridaens, A. Piazza,
Dipartimento di Fisica, University degli Studi di Trento, I -38050 Povo (TN) Italy

3. ABSTRACT

The concept and the realisation of a scanning positron microscope will be shown and discussed. A positron beam with a variable energy from 0.5 to 30 keV, with a spot diameter of 1 μm or below, can be scanned over an area of 0.6 x 0,6 mm^2. This beam is formed after a double stage stochastic cooling (moderation) of the positrons emitted from a radioactive isotope. In addition the positron beam will be pulsed in order to have a well-defined time base for positron lifetime measurements. In the system included is a conventional scanning electron microprobe for surface analysis. The design of the scanning positron microscope is dominated by the special demands of positron physics.

4. INTRODUCTION

Experiments in physics involving the interaction of matter with antimatter are fascinating. Positrons are particles with the same mass as an electron, but with opposite charge. This means that positrons belong to the group of antimatter. Their positive charge makes them very sensitive for changes in the electron density in materials. Positron annihilation has advanced to a standard method for studies of microscopic properties in condensed matter *[1,2]*. The field of low energy positron physics has expanded significantly in recent years. This includes not only particle and atomic physics but most extensively the areas associated with condensed matter and materials science.

The interaction of a positron with solids can be roughly divided into various categories: as electronic structure probes, as lattice defect probes, as surface and interface probes and as microbeam probes. The advances in positron annihilation methodology from the use of a broad inhomogeneous beam of high-energy positrons from radioactive nuclei to a narrow homogeneous beam of monoenergetic positrons of variable energy, expanded the object of studies from only bulk properties to surfaces and depth specified near surface layers and interfaces, and even further to three-dimensionally specified microscopic regions.

During the last several years radio frequency pulsed low-energy positron beams have proved to be a very valuable tool for lifetime spectroscopy in the near surface region [3-5], The underlying principle is to compress a continuous beam of monoenergetic positrons to pulses of about 100 ps width or less at the target position by means of special radio frequency devices. The timing signals for the lifetime measurements are derived from one of the annihilation quanta and the corresponding clock signal of the radio frequency system, respectively [3].

The diameter of the positron beam in this system is about 4 mm [3], Apart from the possibility to perform lifetime measurements as a function of the positron energy and hence the penetration depth of the positron into the specimen, there is another important advantage to conventional lifetime measurements: no restriction of the positron intensity because of accidental coincidences. Since one of the timing signals is taken from the radio frequency system, the final coincidence rate is equivalent to the counting rate of the detector for the annihilation photons (singles rate). This count rate can then be increased almost unlimited if an appropriate intensive primary positron source can be used [6,7]. An almost natural consequence, after the existence of a positron beam of several mm in diameter, is the upgrading step to reduce this diameter into the micrometer region. This leads to the development of a scanning positron microscope, i.e. a pulsed positron beam of variable energy with microscopic dimensions, This scanning positron microscope is a combination of a conventional scanning electron microscope and a pulsed positron microprobe with micrometer spot size and a pulse duration of about 100 ps. In the electron beam mode the surface morphology of the specimen is imaged in the conventional way, Regions of interest in this image can then be selected for a nondestructive defect analysis by the positron microprobe. In the following the basic principle of such a system as well as its technical realization will be discussed.

5. *TECHNICAL DESCRIPTION*

5.1 Basic Principle of the Scanning Positron Microscope

A microscope which is sensitive to defects as small as a single vacancy can only be based on a positron beam system. There are, however, many strategies to form a narrow pulsed positron beam. The present principle and design is based on the experience with positron beams [5] as well as on recent progress in particle optics [8-10]. The fundamental difference between electron and positron beam systems consists in the flux density of its sources. The flux density of a typical LaB6 electron source exceeds the flux density of a monoenergetic positron beam by a factor of 1016, Therefore the probe forming strategy for a scanning positron microscope must be to maintain the positron flux as good as possible, in contrast to the typical probe forming strategy for a scanning electron

microscope which is based on narrow apertures and corresponding intensity losses. This means that the positron remoderation technique has to be applied [2]. The remoderation efficiency is approximately 20°/0 in the reflection mode and only about 10°/0 in the transmission mode. In order to obtain a sufficient event rate with a relatively weak and easy to handle primary positron source, the design is based on only a single remoderation stage in the reflection mode. However, compared to existing positron microbeam systems with remoderation [2, 11] a number of different designs and developments has to be made [12],

5.2 *Technical Realisation*

Introducing the new technique of a scanning positron microscope (SPM) depends on the availability of a first prototype. Therefore the central goal is the development and construction of such a system with micrometer spot size and with a pulsed beam. This is an absolutely novel device without any precursor or technical reference system. The development has to focus on the most critical problems, i.e. sufficient spatial and time resolution, efficient use of the primary positron source, sufficient mechanical and electric stability, safety and an appropriate measuring chamber.

The scanning positron microscope is a self-contained instrument which operates under usual laboratory conditions. The complete system is shown schematically in fig. 1. The entire SPM is designed for best resolution under optimal measuring conditions. The elements for the beam optics have been fabricated with the highest possible precision. The mechanical support is as rigid as possible, however, with unrestricted access to all parts of the system. The entire system is operated under ulta high vacuum conditions in the 10-9 to 10^{-10} mbar range. Specimens of dimensions up to 20 x 20 x 3 mm^3 can be inserted through a lock system. A test specimen (platinum on silicon dioxide) is permanently installed and enables easy alignment and focusing of both the electron and positron image,

Besides of the positron beam also an electron beam is provided which produces a conventional electron image of the specimen surface. The scanned area in the electron and positron mode is at least 600 x 600 μm^2. With the specimen manipulator any region of the specimen can be positioned within the scanned area. The region to be investigated by positrons can be selected in the electron image. For the positron lifetime measurements a fast detector for the annihilation photons is mounted inside the objective lens. This detector can be replaced with a Ge diode for studies of the Doppler broadened annihilation radiation. In this case only a continuous positron beam would be sufficient. In the following the various functional units are discussed separately.

5.2. I *Primary beam*

The source-moderator assembly coupled with a first accelerator produces a continuous positron beam of 20 eV kinetic energy which is injected into the drift tube, A sawtooth signal with a repetition rate of 50 MHz is applied to the drift tube. This compresses the positrons in each 20 ns segment of the beam into bunches with a width of 2 ns (see fig. 2 for the timing. diagram at various points of the SPM). The drift tube compression is much more efficient than the conventional chopping of the beam [13]; about a 3 0°/0 positron loss compared to a 90°/0 loss, respectively. The transport through the drift tube has been achieved with an unusual axial-magnetic-field configuration. A homogeneous axial magnetic field is present along the entire drift space. The operating magnetic field is about 0.5 mT. The guiding field acts like a thick lens and images the entrance of the drift tube onto the exit aperture [14]. The drift tube is constructed in two parts. The direction of the axial field is opposite in these two parts. This avoids image rotation and minimizes the transverse momentum introduced by the axial magnetic field. Field terminators are placed at both ends of the drift tube to avoid magnetic-field leakage out of the drift tube. A third terminator at the center of the drift tube matches the two regions. Positrons leaving the drift space are accelerated up to 800 eV and injected into a 100 MHz sine wave buncher. This buncher has the same design as already used in a previous system [5]. The buncher is a resonant cavity with an active gap and has been designed as a thermally compensated unit. The bunching gap is supplied by a 100 MHz sine wave of about 100 V amplitude. A beam blanker positioned before the entrance to the buncher suppresses the background of positrons outside the prebunched pulse. The main buncher compresses the 2 ns pulses down to 200 ps at the remoderator position.

After the exit from accelerator 4, the positrons drift in field-free space with an “average energy of 5 keV over a distance of 640 mm until they reach the remoderator crystal. The remoderator is mounted inside a cryostat which can be operated at liquid nitrogen temperatures. A single crystal of tungsten oriented along the 100 direction is mounted between two molybdenum pieces. The remoderation efficiency has been measured as (23’ ± 2)%. It is expected that after cooling the tungsten crystal to 100 K the transverse energy spread of the remoderated positrons will be reduced by a factor of three, resulting in a reduction of the final spot diameter by about 40°/0.

The optics of the remoderator unit is a combined electric and magnetic lens system which focuses the incoming parallel positron beam of 5 keV kinetic energy onto the remoderator and which transports also the remoderated positrons as a parallel beam of 200 eV kinetic energy [15, 16].

Because of the ultra high vacuum requirements and in order to have sufficient space for the liquid nitrogen cryostat, a magnetic single pole lens is placed behind the remoderator chamber. Since it is easy to achieve the required focal length and small aberration

coefficients by a magnetic lens, the pole shoe and the magnetic field is optimized with respect to the reemitted positrons. In order to minimize spherical aberrations, the axial field should follow the inverse quare law of a perfect monopole [15], This condition is fulfilled by selecting a conical pole shoe with 20 degree half angle and a central hole to prevent saturation at the tip. In test bench measurements the incoming positron beam could be focused by the lens to 20 µm FWHM.

However, from the known diameter of the incoming beam of 1.5 mm, we expect a spot size of about 10 µm.

5.2.2 *Final* ***Beam***

In order to separate the incoming and the remoderated beam and to direct the latter one to the main optical column, toroidal deflector coils are installed. According to the calculations and all tests during set up, these deflectors have no influence on the quality of the incoming beam which is only displaced by 20 mm. Computer simulations confirm this also for the remoderat ed beam.

At the entrance of the optical column the nominal beam diameter is 1.5 mm with a pencil haIf angle of 10-3. For beam adjustments and as a possible defining aperture precise diaphragms are provided which can be positioned externally.

The remaining parts of the optical column are the accelerator for positron implantation energies from 0.5 to 30 keV (continuously variable), the scanning coils, the specimen chamber and the magnetic probe forming lens.

The accelerator acts as a lens which has to form an intermediate image at a given position and with a given size. However, the important elements vary with the acceleration voltage. Therefore the accelerator is designed as a zoom lens consisting of an einzel lens and two accelerating sections [17]. These interacting lenses are operated in three different modes: In the first mode, for acceleration voltages from 0.5 to 4 keV, the einzel lens is combined with an immersion lens. In the second mode, from 4 to 7 keV, the einzel lens is combined with a four stage accelerator. In the third mode, from 7 to 30 keV, the einzel lens is combined with an eight stage accelerator. The accelerator was analyzed explicitly by ray tracing with the SIMION program [18].

The mechanical design of the accelerator ensures stability under all operating conditions, including bakeout. Therefore the intrinsic column is made out of Macor and molybdenum, which have about the same thermal expansion coefficient. All elements were manufactured with high accuracy, i.e. 10 µm tolerance with respect to rotational symmetry.

At the exit of the accelerator the beam enters a large Faraday cage at the final implantation voltage. Therefore the deflection coils for the magnetic beam scanning are placed outside the vacuum chamber. Finally the beam enters the specimen chamber and the magnetic field of the probe forming lens. Because of the completely different measuring technique with

positrons, this part of the scanning positron microscope must differ completely from the specimen chamber of a scanning electron microscope. In order to obtain a high count rate of the annihilation photons, a radiation detector as large as possible has to be placed as close as possible to the specimen. On the other hand, the half space in front of the specimen must be free of matter in order to suppress the distortion of the lifetime spectra by annihilation radiation resulting from backscattered positrons annihilating at the wall.

The necessary design requirements have been met by a side-gap single-pole lens, placed behind the specimen outside of the vacuum chamber with the radiation detector inside the central pole shoe [16]. The lens has an inner pole shoe diameter of 36 mm with a 3 mm diameter bore and a 45 degree cone for the detector. A double-walled magnetic shielding for the photomultiplier tube is necessary.

The measured magnetic field of the side-gap lens agrees with the calculated one for all excitations. The deviation of the radial field component from the radial symmetry in the plane of the specimen is below the detectable limit of 0.01 mT.

6. *RESULTS*

6. I *Primary beam*

The beam intensity has been evaluated in separate measurements with a specially manufactured radioactive source of 1 mm diameter and a channeltron as a detector. The activity of 0,6 mCi ^{22}Na was deposited on a 1 mm diameter spot. A titanium foil of 5 μm thickness was used to cover the active area. An effective distance of about 0.3 mm between the moderator and the radioactive spot was achieved. In this configuration a 3 mm diameter of moderated positrons corresponds to 30% of the total solid angle of the positrons emitted from ^{22}Na. The efficiency of the channeltron for positrons as a function of the energy was not determined. Rather the measurements by Seah [19] were used to estimate a detection efficiency of 40°/0 at 5 keV positron energy. The detected counting rate was checked to scale with energy in the same way as the efficiency values given in ref. [19].

With a freshly conditioned moderator about 2000 counts/s were obtained at the channeltron. A very reproducible situation, lasting several weeks in a vacuum of 10-9 mbar, yielded 1400 counts/s. This corresponds to an overall yield of more than 5000 e^+/(smCi). Transforming this number into an efficiency, this quantity has to be defined as the product of the moderator efficiency combined with the transport properties of the positron optics. This product is 6 x 10^{-4}. It can be interpreted as produced by a very efficient tungsten moderator of 1 μm thickness ($\varepsilon \geq 6 \times 10\text{-}4$) and a nearly perfect collection and transmission of the reemitted positrons.

In order to measure the spatial resolution at the remoderator position, the remoderator was replaced by a gold grid (360 μm spacing, 30 μm bars), which was positioned at the image plane of the single-pole lens [16]. The beam was allowed to pass through the bore of the lens, Positrons not intercepted by the grid structure were annihilating at the end of the vacuum chamber close to a 3" x 3" NaI(Tl) scintillator. The annihilation photons originating from the grid (50 mm away from the' scintillator) were mainly shielded by the metal structure of the lens. Furthermore, the solid angle for detection of these annihilation photons was smaller so that the counting rate decreased when the positrons annihilated at the grid bars. Fig. 3 shows the first image of the gold grid, obtained by scanning the beam with 300 x 300 pixels resolution under computer control. Also an example of a single-line scan is shown in the insert of fig. 3. A line width of less than 15 μm FWHM can be determined from this line scan and the total spot size is less than 20 μm. The non rectangular distortion of the image is attributed to an imperfect positioning of the test scanning coils, No influence on the spatial resolution was observed *when* the energy modulation for the beam bunching was applied [20].

For the determination of the time resolution, a BaF2 scintillator coupled to a Valvo XP 2020Q photomultiplier was used as radiation detector. The experimental set-up was similar to the one described in ref. [5]. The analysis of the measured positron lifetime spectrum results in a pulse width of 200 ps FWHM at the remoderator position.

6.2 *Final positron and electron beam*

With a measured remoderation efficiency of 23% the phase-space density of the reemitted positrons from this pulsed positron microsource (20 μm spot size) will exceed the one of the first moderator by a factor of about 3 x 104. Up to now, the typical gain in phase-space density of a single remoderation stage was only about 20 [21]. This means that in the scanning positron microscope only one remoderation stage will replace three conventional remoderation stages, reducing the required primary source strength by a factor of 25. This progress is due to the well balanced transport system in the beam, the outstanding properties of the single pole lens and the application of time bunching, which contributes with a factor of more than 50 to the total gain in the phase-space density [20].

The image from the electron beam, which passes the same optical column as the positron beam, is a quick reference for selecting regions of interest for positron studies, for perfect focussing and for alignment of the optical column by adjustment of the current in the correction coils. Since the specimen is biased with high voltage, the electron beam has to be pulsed also at a repetition rate of 20 to 40 kHz in order to measure the primary part of the sample current with a charge sensitive preamplifier. It is also possible to measure the signal induced by secondary electrons of low energy, which gyrate along the magnetic field lines of the objective lens until they reach the gold layer on top of the insulating specimen

holder. Since the backscattered electrons have only a small chance to reach the specimen holder itself, this signal can convey additional information.

During the test phase, the electron beam is also monitored optically by a scintillator crystal which is mounted in the specimen position and covered with a gold mesh of 360 µm pitch and 30 µm bar widths.

In fig. 4 this mesh is shown which has been obtained at an electron beam energy of 7.5 keV and an emission current of 1 µA. Besides of the achieved resolution, also the stability of the electron image as a function of the final beam energy and the perfect matching of the electron and positron images are of particular importance.

At present, the achievable spatial resolution of the positron image has not yet been evaluated experimentally. Therefore the subsequent estimates are based on the evidence from test measurements on the actual performance of the components (e.g. primary beam, remoderator, optical column, axial magnetic, field of the probe forming lenses, etc.). With a 5 mCi commercial ^{22}Na test source (3 mm effective diameter of emitting area at the primary moderator) a beam spot of 20 µm FWHM has been observed in the test measurements [20]. After system integration and some modifications of the primary beam an even better performance was obtained so that a beam spot of about 10 µm FWHM at the remoderator will be produced. The optical properties of the magnetic lenses at the remoderator and-at the specimen positions are very similar. With the remoderator cooled to liquid nitrogen temperature and the final ^{58}Co positron source of 1 mm diameter, this will result in the following predicted spatial resolutions: 0.5 µm FWHM at 1 keV and 0.2pm FWHM at 10 keV positron energy.

The actual remoderation and bunching efficiencies have been determined to 23°A and 70%, respectively. For a primary source of 1 Ci ^{58}Co, this corresponds to about 5.8 x 105 positrons per second at the specimen and an event rate of about 2 x 104 per second for a BaF2 scintillator (efficiency including solid angle is 4%).

7. *CONCLUSIONS*

The presented scanning positron microscope with micrometer resolution and with a pulsed structure is the first operational system of its kind. This system is designed and built not only for demonstration of the principle but also for general applications under normal laboratory conditions.

8. *ACKNOWLEDGEMENTS*

The development of the scanning positron microscope has been supported by the European Community within the Brite/Euram programme with the project number BE 3044 and contract number BREU-CT90-0347 as well as by the Universität der Bundeswehr München.

9. REFERENCES

[1] W. Triftshäuser, Microscopic Methods in Metals (Topics in Current Physics, Vol. 40, Springer, Berlin-Heidelberg-New York, 1986) pp. 249-295

[2] J.P. Schultz and K.G. Lynn, Rev. Mod. Phys. 60 (1988) 701

[3] D. Schödlbauer, P. Sperr, G. Kögel, and W. Triftshäuser, Nucl. Instr. Methods B 34 (1988) 258

[4] R. Suzuki, Y. Kobayashi, T. Mikado, H. Ohgaki, M. Chiwaki, T. Yamazaki, T. Tomimasu, Japan. J. Appl.Phys.~(1991) 532

[5] P. Willutzki, J. Störmer, G. Kögel, P. Sperr, D.T. Britton, R. Steindl and W. Triftshäuser, Meas. Sci. Technol. 5 (1994) 548

[6] W, Triftshäuser, G. Kögel, K. Schreckenbach and B. Krusche, Helv. Phys. Acts 63 (1990) 378

[7] W. Triftshäuser, Journ. Physique IV, Vol. 5 (1995) C2-217

[8] H. Rose, Optik 33 (1971) 1

[9] A.V. Crewe, D. Kopf, Optik~(1980) 1

[10] T. Mulvey, Magnetic Electron Lenses, ed. P.H. Hawkes (Springer, Berlin-Heidelberg-New York, 1982) p. 359

[11] G.R. Brandes, K.F. Canter, T.N. Horsky and P.H. Lippel, Rev. Sci. Instrum. 59 (1988) 228

[12] K. Uhlmann, W. Triftshäuser, G. Kögel, P. Sperr and D.T. Britton, Fresenius Analyt. Chem., in press

[13] P. Sperr, M.R. Maier and P. Willutzki, Mat. Sci. Forum 175-178 (1995) 125

[14] 0. Klemperer, Electron Optics, 3rd edition (Cambridge 1971) p. 108

[15] K. Uhlmann, D.T. Britton, G. Kögel, Optik 98 (1994) 5

[16] K. Uhlmann, D.T. Britton and G. Kögel, Mess. Sci. Technol. 6 (1995) 932

[17] D.T. Britton, K. Uhlmann, G. Kögel, Appl. Surf Science 85 (1995) 158

[18] D.A. Dahl and J.E. Delmore, Electrostatic Lens Analysis and Design Program SIMION, version 4.0, 1988

[19] M.P. Seah, J. Electron Spectrosc. Relat. Phenom.~(1990) 137

[20] A. Zecca, R. S. Brusa, M.P. Duarte-Naia, G.P. Karwasz, J. Peridaens, A. Piazza, G. Kögel, P. Sperr, D.T. Britton, K. Uhlmann, P. Willutzki and W. Triftshäuser, Europhys. Lett. 29 (1995) 617

[21] K.F. Canter, G.R. Brandes, T.N. Horsky, P.H. Lippel, in Atomic Physics with Positrons ed. by J.W. Humberton and E.A.G. Armour (Plenum Press, New York 1987) pp. 153-160

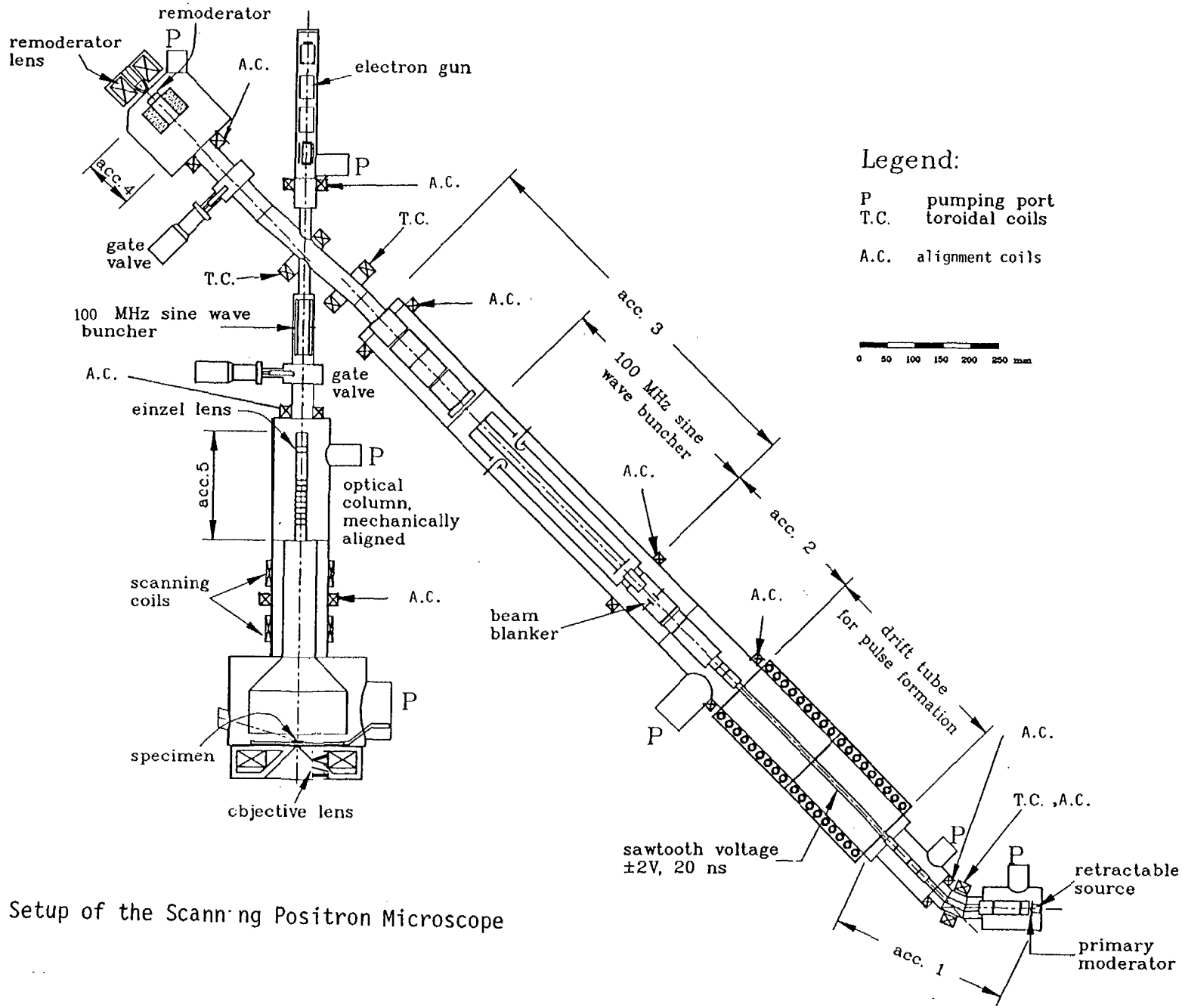

Fig. 1 : Setup of the Scanning Positron Microscope

RMID-F1.DWG 20.4.93 scale 1:10

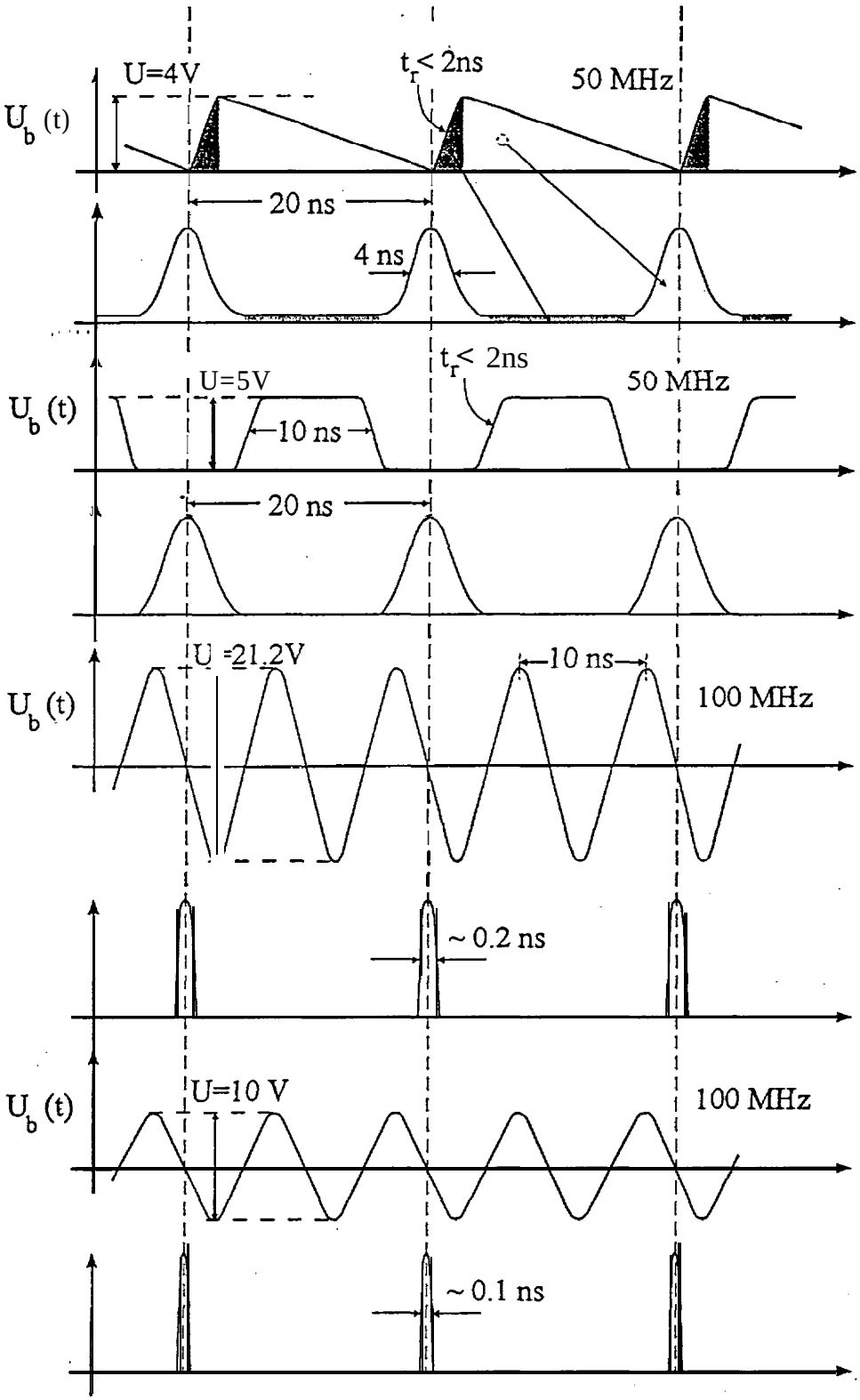

Fig. 2: Timing diagram of the positron beam (from top): sawtooth signal in the drift tube; pre–bunched beam at the entrance of the blanker; rectangular signal to the blanker; beam at the entrance to the main buncher; 100 MHz sine wave to the buncher; beam structure at the remoderator; 100 MHz sine wave to the post buncher; beam structure at the specimen.

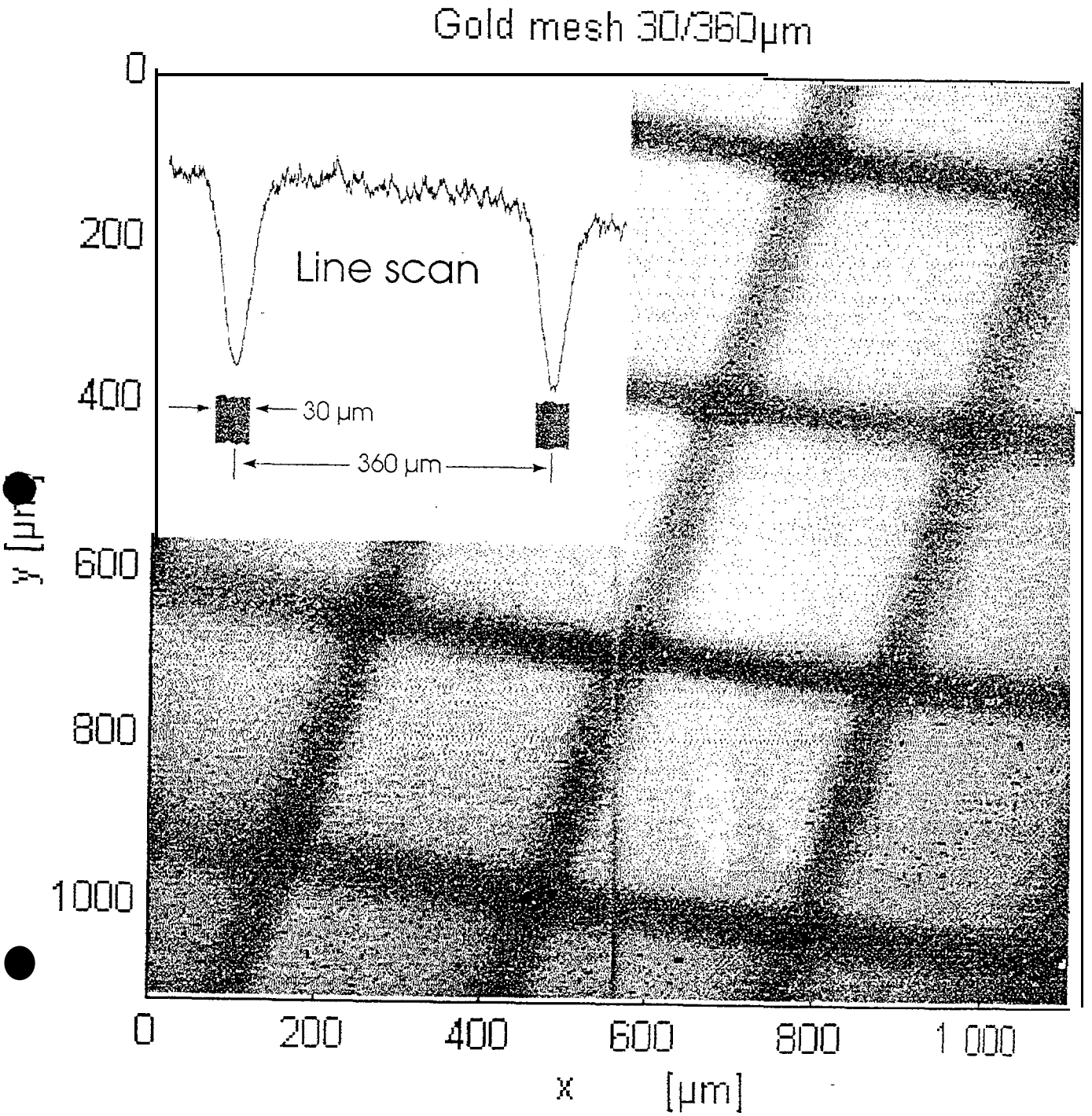

Fig. 3: Positron image obtained by the primary beam of *a* gold mesh of 360 µm spacing and 30 µm bar width, placed at the remoderator position.

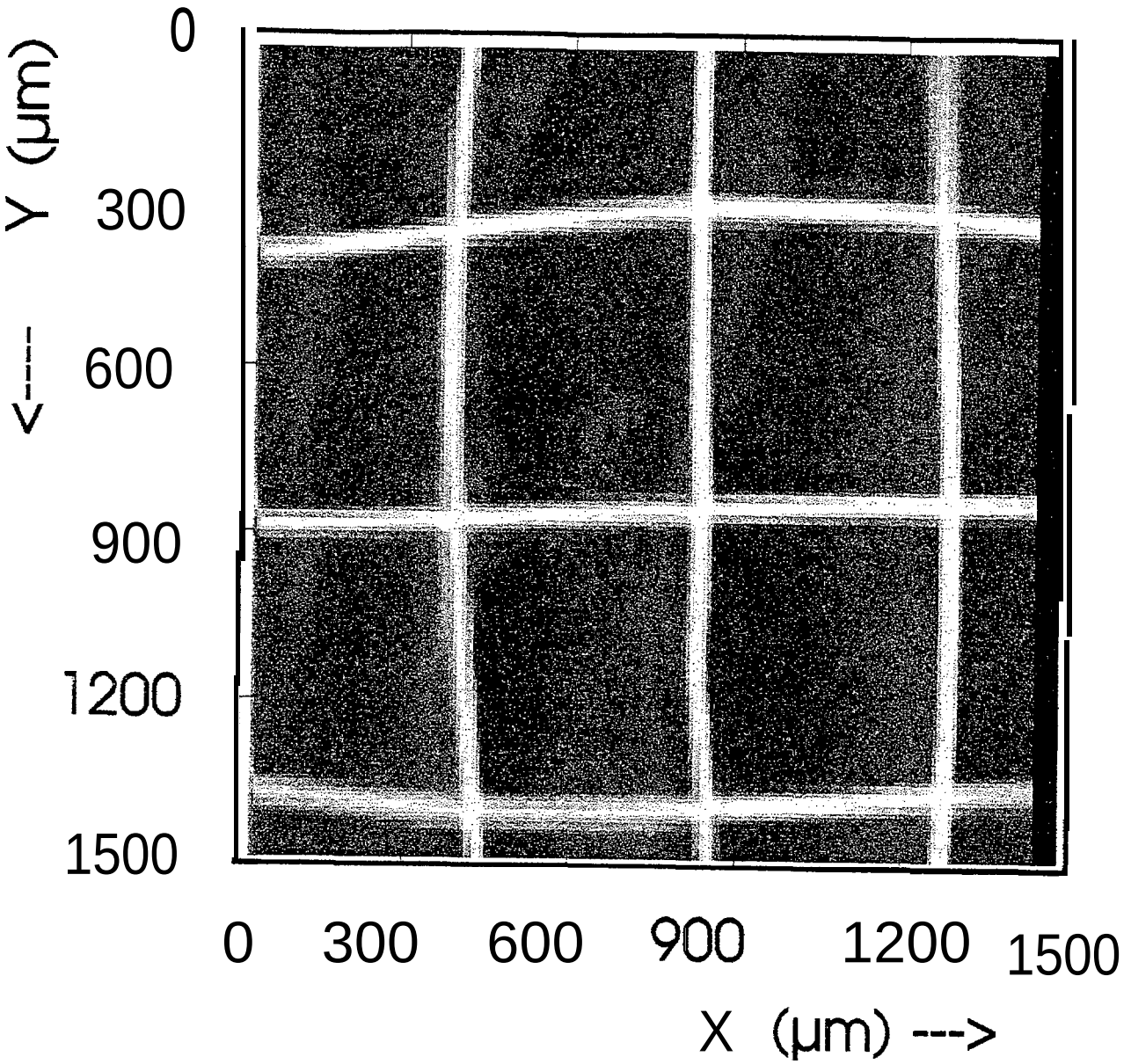

Fig. 4: Electron image of a gold mesh with 360 µm spacing and 30 µm bar width